

THERMAL ANALYSIS FOR DIFFERENT TYPES OF PV PANELS

C. Dainese, R. Faranda, S. Leva
Politecnico di Milano – Department of Energy
Via La Masa, 34 - 20156 Milano
Italy

Email addresses: carlotta.dainese@gmail.com, roberto.faranda@polimi.it, sonia.leva@polimi.it

ABSTRACT

The paper presents a preliminary study of the thermal behavior of different types of photovoltaic (PV) panels. In particular in the paper the traditional panel (non-architectonic PV panel), the architectonic PV panel and a innovative PV panel, which adopts a liquid cooled, are compared in order to evaluate their thermal performance. Thermal models and equivalent thermal networks of each PV panel belonging to the aforementioned categories has been developed to evaluate the thermal behavior in steady state conditions for a specific and constant irradiance and environment temperature values.

The thermal transmittance and the operative temperature of the PV cell of each PV panel are computed and compared. in order to put in evidence the thermal performances of the PV panels and to highlight the highest performances of liquid cooled panels with respect to traditional ones.

KEY WORDS

Photovoltaic Conversion, Thermal Analysis, Liquid Cooled PV Panels, Equivalent Thermal Network.

1. Introduction

Photovoltaic conversion for energy production is a key choice for a strategic and valuable increase in exploitation of clean and renewable energy within the global energy market. However, when compared to expected potentialities, the actual diffusion of PV systems is still strongly limited by several practical factors, e.g. the need for large surface availability for energy production on large scale, the high cost of silicon and PV materials, and the yield degradation, which determines higher costs compared to conventional solutions and introduces long term reliability uncertainties [1].

A solution could consist in concentrating large plants in those areas characterized by high solar irradiation, such as low latitude regions of the globe, coasts and deserts. Most of these areas belong to developing countries, and the diffusion of PV plants in such a context can have a remarkable socio-economic impact while respecting the environment and promoting the technological transfer [2],[3].

High solar irradiation represents a benefit for photovoltaic conversion, but it is also connected with hostile climate conditions, e.g. high temperature and high day-night thermal excursion. The currently commercially available PV panels are designed for mild climate conditions and are not sufficiently reliable under the extreme conditions of the aforementioned applications. For this main reasons, it becomes necessary to develop innovative PV panels able to work with high efficiency in extreme condition behavior. A PV panel equipped with proper cooling systems to keep the temperature low could be a possible solution.

The success of a PV panel with an integrated cooling system depends on the detailed knowledge of the numerous physical phenomena that interact together. All of these effects have to be included in an accurate multi-physics model.

In this paper a preliminary study of the thermal behavior of different types of photovoltaic panels is presented. In particular are compared the performances of non-architectonic PV panel, architectonic PV panel and the innovative PV panel. In order to understand the real PV panel operating conditions the authors have carried out a study considering some figures of merit, i.e. the thermal transmittance and PV cell operative temperature, to highlight the highest performances provided by liquid cooled panel technology with respect to traditional ones.

The results have been then compared with the ones obtained by exploiting the certification test procedure for the same PV panels.

2. Thermal model of PV panels

Incident solar radiation on a PV module is partially reflected and adsorbed by the glass and other material layer placed above the PV cell; the remaining percentage of solar radiation is transmitted to the PV cell which adsorbs it. Only a given fraction of this energy is then directly converted into electrical energy, while the residual fraction is converted into heat [4].

Thermal energy generated by the PV cell is transmitted by radiation and convection to the surrounding environment through front and rear PV module surfaces. The contribution associated to heat transmitted by conduction

to the sustaining structure is instead negligible, due to the fact that the contact area is very small.

The operating cell temperature therefore depends on the absorption of radiation, the cell efficiency, the thermal properties of the module, the environmental conditions (as wind and ambient temperature) and the installation configuration.

A one-dimensional heat transfer model has been developed to simulate the cell operating temperature associated to different types of photovoltaic panels, and it is presented and discussed in the following. In particular, the analysis of the thermal behavior of the various PV panels is performed in steady-state conditions, assuming that the temperature is uniform in the different layers which constitute the panel.

This paper is focused on three panel typologies among the ones available off the shelf:

- traditional PV panel for non-architectonic application;
- PV panel for architectonic applications;
- innovative PV panel provided with cooling liquid.

2.1 Description of the models

The single components that constitute the thermal model are recalled in the following [4].

The conductive heat transfer occurs from different solid material closer between them (i.e. EVA, glass, tedlar, ect...). The thermal resistance R_{COND} to conductive heat transfer can be computed as follows:

$$R_{COND} = s / \lambda$$

where, s is the thickness of the conducting material and λ is the thermal conductivity of conducting materials.

Convective heat transfer occurs from the front and the rear surfaces of the PV module to the surroundings. The thermal resistance R_{CONV} to convection heat transfer depends on the convective heat transfer coefficient α_{CONV} of the material, and it is computed as follows:

$$R_{CONV} = 1 / \alpha_{CONV}$$

where, α_{CONV} depends on various parameters such as air velocity, ambient temperature, and air properties at a given temperature. The dimensionless *Nusselt* number can be used to calculate the coefficient α_{CONV} of convective heat transfer as:

$$\alpha_{CONV} = Nu \cdot \lambda / L$$

where, L is the characteristic length. The *Nusselt* number can be found for a flat plate at different orientations as well as under forced and free convection in many heat transfer reference papers and text books [4].

The radiative heat flows from the front and back surfaces to the surroundings. The expression of the resistance R_{RAD} to radiative heat transfer can be obtained from the standard equation for radiation heat transfer:

$$R_{RAD} = 1/\alpha_{RAD} = 1/\left[\varepsilon \cdot \sigma \cdot (T_s^2 + T_A^2) \cdot (T_s + T_A)\right]$$

where, T_s and T_A are the surface and ambient temperatures respectively, ε is the emissivity of the materials, and σ is the *Stefan-Boltzman* constant.

The heat dissipation P_r , that represents the amount of heat flow from the cell Q_{IN} , is symbolized by a current source. This contribution depends on thermal and optical properties of the cell and encapsulant materials, the illumination intensity and the environmental conditions of ambient air temperature and wind speed. The ambient temperature at the front (T_{Af}) and rear (T_{Ar}) surfaces are instead represented by two different voltage sources.

Generally, the calculation of resistance to convection and radiation heat transfer requires the knowledge of the temperature on the cell layer and on front and back surfaces. Therefore, the model here presented works in iterative way: it requires the initial temperatures of the front and back surfaces in order to calculate the total resistance. The amount of heat dissipation in each direction can be determined from the total resistance, and then, the temperature corresponding to each intersection and to the external surfaces can be calculated. The initial temperatures are corrected until they are equal to the output temperatures.

2.2 Basic assumptions

The convective and radiative coefficients are very difficult to identify correctly, and therefore - in order to compare the different types of panels - the value here determined are based on the reference literature in this field [5]-[9] and exploiting the following assumptions:

- convective heat transfer coefficient of front surface is assumed to be equal to 10 W/(m²·K) for all the three PV panels here considered (it is correlated to forced convection, and hence it is characterized by a very slight dependence on the panel geometry);
- convective heat transfer coefficient of rear surface is assumed to be equal to 3 W/(m²·K) for both the architectonic and the traditional panels, which are characterized by the same geometry;
- convective heat transfer coefficient of rear surface for the innovative PV panel is assumed as a function of the convective heat transfer coefficient for traditional panels and of the characteristic dimensions of the modules by means of the following relation:

$$\alpha_{CONVS} = \alpha_{CONVT} \cdot L_S / L_T$$

where S refers to the innovative PV panel and T refers to the tradition panel.

- radiative contribution of rear surface - identified by the radiative heat transfer coefficient α_{RAD} - has been computed and it results to be equal to 4.5 W/(m²·K) for the rear surface with glass plate;

- radiative contributions of rear surface when tedlar and steel layers are used instead of the glass one, are computed as a function of radiative heat transfer coefficient - for the configuration with the glass plate - and of the emissivity of the materials by means of the following formula:

$$\alpha_{RADx} = \alpha_{RADg} \cdot \varepsilon_x / \varepsilon_g$$

where x refers to tedlar and steel, while g refers to glass.

3. Traditional PV panels (non-architectonic applications)

Photovoltaic modules for most common applications are composed by 48-72 series cells, which allow the coupling with nominal $12V_{cc}$ accumulators. Panels are assembled by connecting and welding the cells among each other by means of terminals on front and rear contacts (in a N-P-N-P-N... sequence) in order to form a string.

A sandwich is then realized by placing the PV cell in the middle layer that is surrounded by - going from the external layer to the internal one - a glass plate characterized by very high transmittance and good mechanical resistance, an EVA (Ethylene Vinyl Acetate) sealant sheet which allows the dielectric insulation of the cell layer, then another EVA sheet and then a tedlar insulant layer.

The sandwich is then heated in the oven at about $100^{\circ}C$, the temperature at which the components seal to each other. Once this temperature is reached, EVA becomes transparent and the residual internal air, which might cause corrosion because of the presence of water vapor, is then evacuated. Eventually, the sandwich is fixed in an extruded anodized aluminum frame - in order to be protected against corrosion - and the junction box is disposed. Typically the shape of these PV panel is rectangular (Fig. 1).

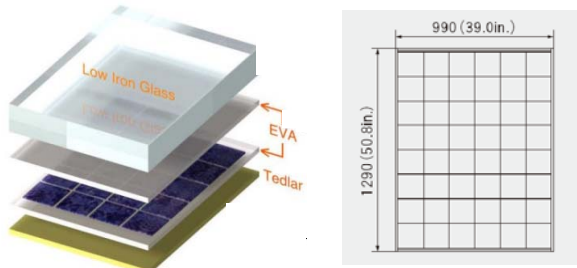


Fig. 1. Typical PV panel with tedlar layer

The PV panel here considered is schematized in Fig. 2, while transversal dimensions are reported in Table 1. The equivalent thermal network of PV panels for non-architectonic applications is reported in Fig. 3.

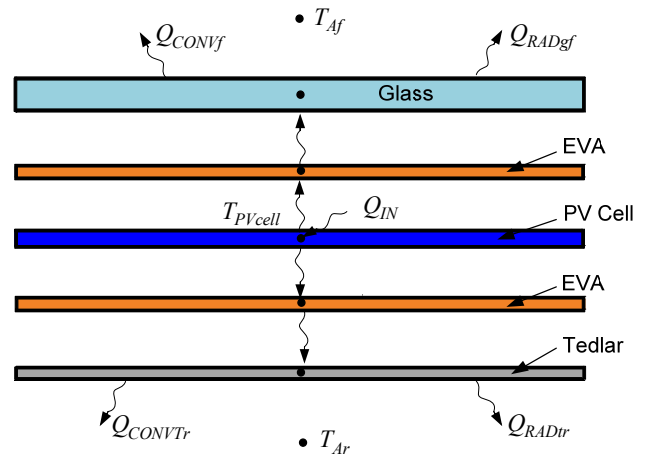


Fig. 2. Transversal section of a typical PV panel with tedlar layer.

Table 1. Transversal characteristic dimensions of traditional PV panel for different layers

Layer	s [mm]
Glass	4
EVA	0.5
Tedlar	0.5
PV cell	0.3

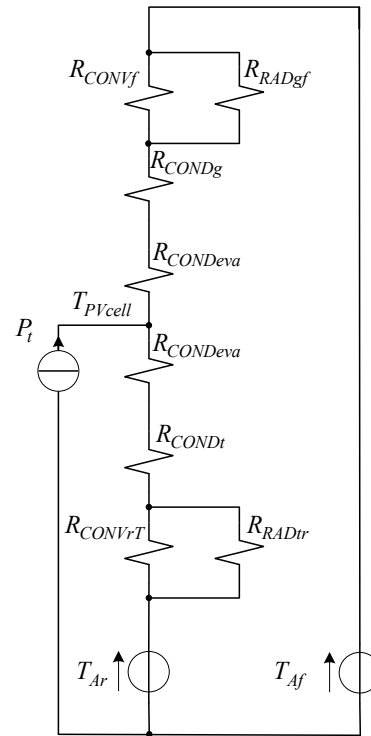


Fig. 3. Thermal network for heat transfer analysis of traditional PV panel for non-architectonic applications

The network include a current generator (P_t), which represents the heat generated by the PV cell, and two voltage generators (T_{Af} and T_{Ar}) which represent respectively the environment temperature corresponding to the front and to the rear side of this PV panel. Eventually the thermal resistances terms are the following:

- glass (v), EVA (eva) and tedlar (t) conduction

resistance ($COND$); the thermal resistance of the PV cell is negligible as it is several orders of magnitude smaller than the other ones;

- convection resistance ($CONV$) of front surface (f) and rear surface to ambient for traditional panels (rT);
- radiation resistance (RAD) of front glass layer to ambient (gf) and of rear tedlar layer to ambient (tr).

4. PV panels for architectonic applications

Photovoltaic modules for most common architectonic applications are realized with the same approach of the ones described above.

In particular the second glass layer is used when the transparency of PV panels is required (Fig. 4).



Fig. 4. Typical PV panel for architectonic applications

Fig. 5 shows the PV panel scheme, while the transversal characteristic dimensions are reported in Table 2.

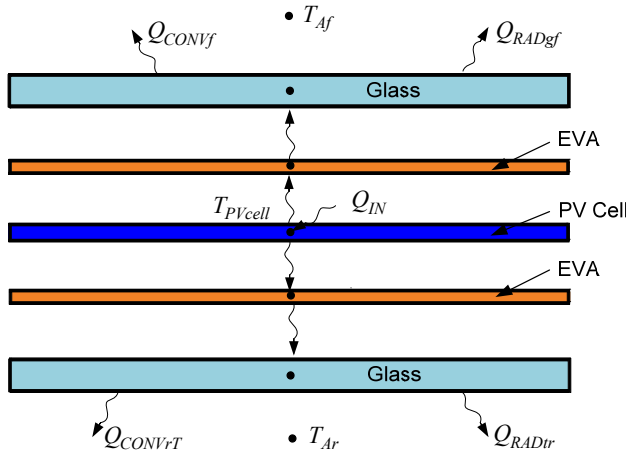


Fig. 5. Transversal section of a typical PV panel with double glass layer for architectonic applications.

Table 2. Transversal characteristic dimensions of traditional PV panel for architectonic applications for different layers

Layer	s [mm]
Glass	4
EVA	0.5
PV cell	0.3

The equivalent thermal network of this PV panel for non-

architectonic applications is reported in Fig. 6. It is analogous to the previous one; the unique difference consists in the value of glass conduction resistance which substitutes the tedlar layer on the rear side of the PV panel.

The value of the radiation of the rear side is equal to the one of the previous panel type, because the glass emissivity is the same to the tedlar one.

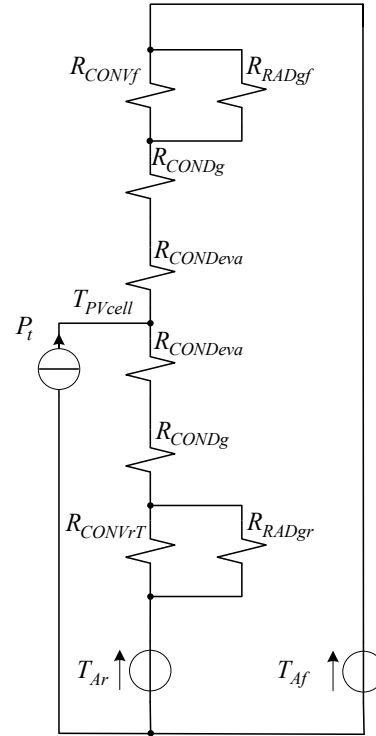


Fig. 6. Thermal network for heat transfer analysis of PV panels for architectonic applications.

Furthermore, as the configuration of the panel here considered is the same of the one described in the previous section (see Fig. 2 and Fig. 5), the value of convective heat transfer coefficient of rear surface to ambient is the same, too.

5. Innovative PV panel with liquid coolant

This type of panel can be schematized as shown in Fig. 7 [10]. This PV panel is constituted by a “case” filled with a light permeable cooling liquid, in which traditional silicon cells are placed in full immersion.

Differently from previous described modules, the insulant EVA layer is not present: it is substituted by the cooling liquid; moreover the second insulant layer is constituted by polypropylene and cooling liquid, and the second glass (or tedlar) layer is substituted by steel. The single PV panel is constituted by 9 polycrystalline silicon cells connected in series, with a total maximum power of 32.9Wp. Furthermore, these panels are characterized by a different geometry with respect to common PV panels as

it can be seen in Fig. 8.

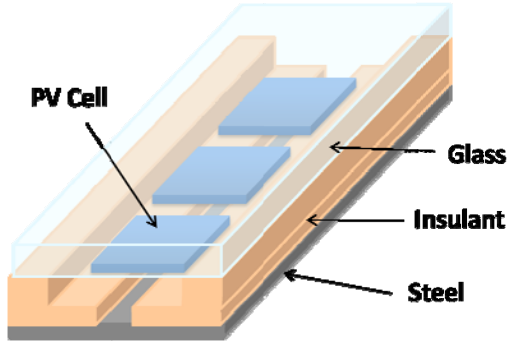


Fig. 7. Scheme of the innovative PV panel

The thermal network is characterized by some differences with respect to the ones shown in the previous sections; some differences are of structural nature, while others are associated to the values of thermal resistances.

In particular, the EVA resistances are substituted by:

- a resistance due to the cooling liquid layer on the front side (R_{CONDlf});
- a resistance due to the cooling liquid layer on the rear side (R_{CONDlr});
- the resistance of the polypropylene insulant (R_{CONDp}).



Fig. 8. In foreground liquid cooled PV panels.

The PV panel here considered is schematized in Fig. 9, while the transversal characteristic dimensions are reported in Table 3, and the equivalent thermal network is shown in Fig. 10.

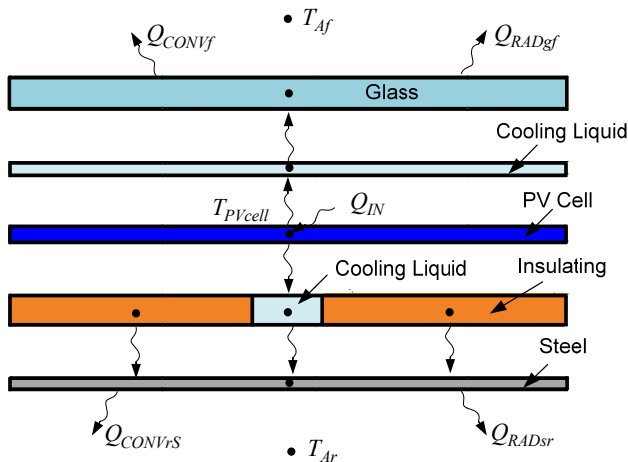


Fig. 9. Transversal section of the liquid cooled PV panel

Table 3. Transversal characteristic dimensions of the innovative PV panel for different layers

Layer	s [mm]
Glass	4
Front liquid	0.7
Rear liquid	3.7
Polypropylene	3.7
Steel	0.4
PV cell	0.3

The thermal flux on the rear surface is opposed by an equivalent thermal resistance which depends on the thermal resistance of the single materials and on the area occupied by them.

Furthermore, the conduction resistances of rear glass and tedlar layers are substituted by the conduction resistance of steel (R_{CONDs}), which is orders of magnitude smaller of them. The value of the radiation of the rear side is equal to the one of the previous panel type because the emissivity of glass and steel is the same.

Eventually, the thermal convection resistance for the rear surface (R_{CONVrs}) is 3-4 times lower with respect to the other cases described above, as the geometry of the liquid cooled panel is very different from the one of traditional panels.

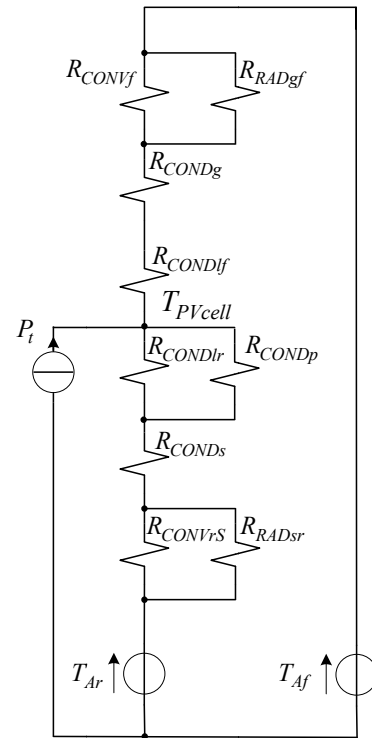


Fig. 10. Equivalent thermal network for heat transfer analysis of the innovative PV panel.

6. Thermal transmittance computation

The thermal transmittance (U) of the different panels is computed using the following formula:

$$U = \frac{1}{\frac{1}{\alpha_{CONVf}} + \sum \frac{s_j}{\lambda_j} + \frac{1}{\alpha_{CONVrY} + \alpha_{RADxr}}} \quad [\text{W/K} \cdot \text{m}^2]$$

where:

- s_j is the thickness of the j^{th} layer;
- λ_j is the conductivity of the j^{th} layer;
- α_{CONVf} is the convective heat transfer coefficient of the front surface to ambient;
- α_{CONVrY} is the convective heat transfer coefficient of the rear surface to ambient for traditional panels ($Y=T$), or innovative ones with cooling liquid ($Y=S$);
- α_{RADxr} is the radiative heat transfer coefficient of the material x on rear surface to ambient.

Regarding the innovative PV panel, no convective motion of cooling liquid has been considered so far; see Section 8 for further considerations.

Moreover, as the cooling liquid occupies only a part of the lower layer of the cell, in the computation of the thermal transmittance an equivalent resistance has been considered: it is obtained by using the corresponding areas as weighting factor for the thermal resistances of the different materials.

Results obtained for the different PV panels here described are shown in Table 4.

Table 4. Thermal transmittance for the different PV panel types

Panel type	Thermal transmittance [W/m ² ·K]
Traditional panel for non-architectural applications	4.149
Panel for architectural applications	4.092
Innovative liquid cooled panel	5.323

The Table 4 shows that the innovative PV panel is characterized by the highest thermal transmittance, and hence a highest transmitted/wasted heat ratio at each point in time. This is mainly due to the fact that the convective resistance of rear surface with surrounding environment for the innovative PV panels is about 3–4 times lower than the one for traditional panels.

7. Operative temperature computation

The operative temperature of PV cells for the different panel types here considered is based on the following measured values of environment temperature and thermal power, reported also in [8], using the Standard Test Conditions (STC) as a reference (temperature in shadow: 25°C, irradiance: 1000W/m², and AMSD: 1.5):

- environment temperature on front side $T_{Af}=31.7^\circ\text{C}$;
- environment temperature on rear side $T_{Ar}=25^\circ\text{C}$;
- thermal power generated by the cell and converted in heat $P_f=550 \text{ W/m}^2$.

The values of thermal resistances exploited for the computation of the thermal transmittance have been used,

and an iterative model for a very precise computation of the PV cell temperature has been developed by considering the non-linearity of radiation coefficients as a function of the temperature.

The results are summarized in Table 5.

Table 5. PV cell operative temperature for different panel types

Panel type	Temperature [°C]
Panel for non-architectural applications	58
Panel for architectural applications	58.5
Innovative liquid cooled panel	53.9

These results show that the PV cells of the innovative PV panel operate at a temperature that is about 4-5°C lower than the one of traditional panels, being equal all the operative conditions. This is mainly due to the geometry of the system which causes the convective heat transfer coefficient corresponding to the rear surface to be about 4 times higher than the one of traditional panels.

8. Influence analysis of the convection of cooling liquid

The computation of the convective heat transfer coefficients - both the ones corresponding to heat transfer to surroundings and the ones corresponding to the internal fluid - represents one of the key issues in heat transmission research field.

Usually they are preliminary estimated and then values are tuned by exploiting experimental data for the specific application under analysis.

Concerning the innovative PV panels, in the previous sections they have been modeled by considering only the value of the thermal conductivity of the liquid, but the convective coefficient might be up to 20 times larger than the thermal conductivity term. This value depends on the physical characteristics of the fluid, on the difference between the temperature of the surrounding layers, and especially on the thickness of the layer filled with the fluid.

Table 6 summarizes the PV cells operative temperature of the innovative PV panel corresponding to different values of the Nusselt number for the liquid placed on the rear side of the panel (all the other conditions are equal to the ones mentioned in the previous section).

Table 6 shows that the operative temperature of the PV cells for liquid cooled panels can be further reduced of about 4-5 °C if the natural convection of the cooling liquid is taken into consideration.

Fig. 11 shows the correlations between PV cells operative temperature and environment temperature when irradiance on panels is 1000W/m².

The Nominal Operating Cell Temperature (NOCT), in case of irradiance equal to 800 W/m², results to be 41.3°C.

Table 6. PV cell operative temperature for the innovative PV panel as a function of the *Nusselt* number.

<i>Nusselt</i> number	Temperature [°C]
1	53.9
2	51.37
3	50.44
4	49.96
5	49.67
6	49.47
7	49.32
8	49.22
9	49.13
10	49.07

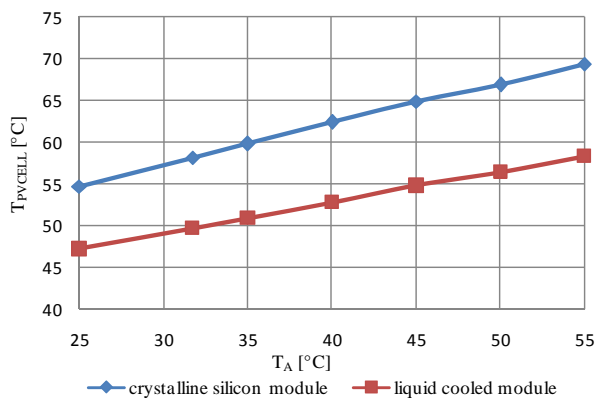


Fig. 11. Cell temperature for a traditional PV module and for an innovative one as a function of environmental temperature

The certification tests performed on the panels in a qualified external laboratory resulted in a maximum-power temperature coefficient for a crystalline silicon module equal to $-0.149 \text{ W}/^\circ\text{C}$ [11]. At Standard Test Conditions the maximum power coefficient for crystalline silicon modules ranges between $-0.3 \text{ W}/^\circ\text{C}$ and $-0.45 \text{ W}/^\circ\text{C}$. The measured NOCT is $38.5 \pm 4 \text{ }^\circ\text{C}$; NOCT for crystalline silicon modules ranges between $43 \text{ }^\circ\text{C}$ and $55 \text{ }^\circ\text{C}$ [11].

9. Conclusion

The analysis here presented shows that the thermal transmittance of PV panels with liquid coolant is higher than the one of traditional panels. Furthermore, being higher both the thermal transmittance and the flux of wasted heat, the liquid cooled panels can be characterized by a cell operative temperature that is up to ten times lower than the one of PV cells in traditional panels. The high flux of wasted heat in the innovative panels here discussed is due both to the exploitation of the liquid

coolant and to the particular geometry adopted.

These results here presented should be considered as a first step to be followed by more accurate analysis both at simulation and laboratory level. It is expected to be very useful to perform an experimental analysis by means of thermal probes placed on the front and rear surfaces of the different PV panels aimed at computing the convective and radiative heat transfer coefficients in the different cases.

Anyway, regarding the innovative PV panel, the obtained results show a great agreement with the data obtained by means of the certification test of the PV panel performed by an external laboratory. Nevertheless, in order to verify the results here obtained and to tune the convective heat transfer coefficient values associated to the fluid, it is necessary to carry out some measurement putting thermal probes on the rear side of the cell and then perform tests with and without the liquid coolant.

In order to complete the analysis and evaluating with higher accuracy the operative temperature of the PV cells, a model capable of simulating the electrical behaviors of the cell itself is going to be developed.

References

- [1] <http://re.jrc.ec.europa.eu/pygis/>
- [2] K. Komoto, P.van der Vleuten, D. Faiman and K. Kurokawa, *Energy from the Desert: Feasibility of Very Large Scale Photovoltaic Power Generation (VLS-PV) Systems*, James & James Ltd., London, 2003
- [3] K. Komoto, P.van der Vleuten, D. Faiman and K. Kurokawa, *Energy from the Desert: Practical Proposals for Very Large Scale Photovoltaic Systems*, James & James Ltd., London, 2006
- [4] F.P. Incropera, D.P. De Witt, T.L. Bergman, A.S. Levine, *Fundamentals of Heat and Mass Transfer*, 6th ed., John Wiley & Sons, 2007
- [5] W.P. Wah, Y. Shimoda, M. Nonaka, M. Inoue, M. Mizuno, *Field Study and Modelling of Semi-Transparent PV in Power, Thermal and Optical Aspects*, Journal of Asian Architecture and Building Engineering, Vol.4, No.2, November 2005, pp.549-556
- [6] K. KC, K.R. McIntosh, B.S. Richards, V. Everett, *A Thermal Comparison of Silver® and Conventional Silicon Photovoltaic Modules*, Clean Energy? – Can Do! – ANZSES 2006
- [7] H.A. Zondag, D.W. de Vries, W.G.J. van Helden, R.J.C. van Zolingen, A.A. van Steenhoven, *The yield of different combined PV-thermal collector designs*, Solar Energy, Vol. 74, 2003, pp. 253–269
- [8] D. Infield, L. Mei, U. Eicker, *Thermal performance estimation for ventilated PV facades*, Solar Energy, Vol. 76, 2004, pp. 93–98
- [9] G.M. Tina, S. Scrofanì, *Electrical and Thermal Model for PV Module Temperature Evaluation*, Proc. 14th IEEE Mediterranean Electrotechnical Conference (MELECON), 5-7 May 2008, pp. 585-590
- [10] G. Carcangiu, I. Carcangiu, *Innovazione nei pannelli solari, pannelli solari fotovoltaici e simili*, Ufficio Italiano Brevetti e Marchi n.01306824, 2001– In italian
- [11] D. L. King, J. A. Kratochvil, W. E. Boyson, *Temperature coefficients for PV modules and arrays: measurement methods, difficulties and results*, Proc. 26th IEEE PVSC Anaheim, CA, 1997, pp. 1183-1186